Journal Pre-proof

AC Electrohydrodynamic Propulsion and Rotation of Active Particles of Engineered Shape and Asymmetry

Nidhi M. Diwakar, Golak Kunti, Touvia Miloh, Gilad Yossifon, Orlin D. Velev

PII: \$1359-0294(22)00025-5

DOI: https://doi.org/10.1016/j.cocis.2022.101586

Reference: COCIS 101586

To appear in: Current Opinion in Colloid & Interface Science

Received Date: 12 December 2021
Revised Date: 25 January 2022
Accepted Date: 11 March 2022

Please cite this article as: Diwakar NM, Kunti G, Miloh T, Yossifon G, Velev OD, AC Electrohydrodynamic Propulsion and Rotation of Active Particles of Engineered Shape and Asymmetry, *Current Opinion in Colloid & Interface Science*, https://doi.org/10.1016/j.cocis.2022.101586.

This is a PDF file of an article that has undergone enhancements after acceptance, such as the addition of a cover page and metadata, and formatting for readability, but it is not yet the definitive version of record. This version will undergo additional copyediting, typesetting and review before it is published in its final form, but we are providing this version to give early visibility of the article. Please note that, during the production process, errors may be discovered which could affect the content, and all legal disclaimers that apply to the journal pertain.

© 2022 Elsevier Ltd. All rights reserved.

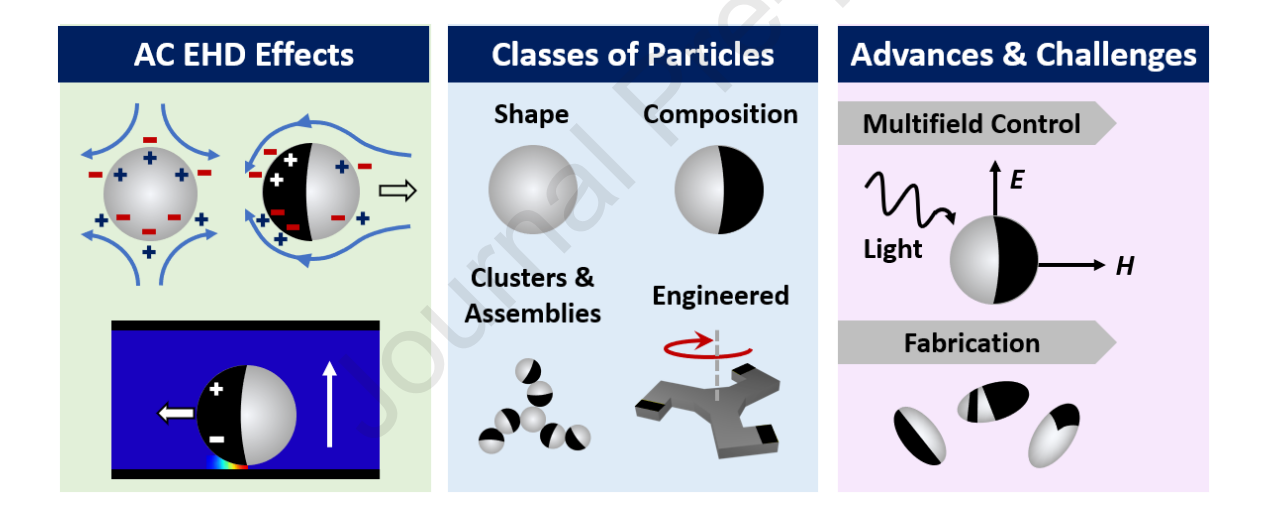


AC Electrohydrodynamic Propulsion and Rotation of Active Particles of Engineered Shape and Asymmetry

Nidhi M. Diwakar^{1†}, Golak Kunti^{2†}, Touvia Miloh³, Gilad Yossifon^{2,3}, Orlin D. Velev^{1*}

Nidhi M. Diwakar: nmdiwaka@ncsu.edu, Golak Kunti: golakme@gmail.com Touvia Miloh: miloh@tauex.tau.ac.il, Gilad Yossifon: gilad.yossifon@gmail.com

*Orlin D. Velev: odvelev@ncsu.edu



Abstract

This review presents the recent progress in the development of active particles driven by alternating-current (AC) electrokinetic effects. These particles propel by asymmetrically dissipating the external energy provided by the fields. An AC field can trigger several electrohydrodynamic mechanisms depending on the field frequency and amplitude, which can also control particle-particle interactions and collective behavior. Recently there has been a strong focus on powering and controlling the motion of self-propelling particles with engineered shape, size, and composition. We introduce a tiered classification of AC field-driven active particles and discuss the fundamental electrohydrodynamic effects acting in individual and multi-particle systems. Finally, we address the limitations and challenges in the current state of AC-field driven engineered particles.

¹ Department of Chemical and Biomolecular Engineering, North Carolina State University, Raleigh, NC 27695–7905, USA.

² Faculty of Mechanical Engineering, Technion – Israel Institute of Technology, Haifa 32000, Israel

^{2, 3} School of Mechanical Engineering, University of Tel-Aviv, Tel-Aviv 69978, Israel

[†] These authors contributed equally.

Keywords: Induced charge electrophoresis, active particles, AC field, self-electrophoresis

1. Introduction

Active particles or "micromotors" are a class of microscale entities that harvest energy from external sources and dissipate it directionally, resulting in their net propulsion. In most cases, the motion is generated due to symmetry breaking in particles' shape, size, or composition, directing the external energy into kinetic motion. Through theory, simulations and experiments, researchers have studied extensively the self-propulsion and assembly behavior of anisotropic spherical colloids, such as spherical Janus Particles (two-faced particles, abbreviated JP) [1–16] that enable control over their self-propelling behavior as well as collective effects [17–25]. As this research field has matured and expanded, researchers have introduced novel classes of particles with complex designed shape and composition, many of them resulting from advances in micro- and nanofabrication [26]. Such particles include, for example, dimers [34], chiral and shaped clusters [11,28], gear-shaped micro-objects, and super-colloidal spinners and motors [30-34].

Active particles can be defined as ones that harvest the energy provided by external fields traversing their medium and convert it into directional motion by means of locally induced gradients coupled to energy dissipation into the surrounding fluid [35]. Such particles can be energized by several physical mechanisms, where the energy needed for propulsion is provided by light, catalytic reactions, magnetic fields, ultrasound, or electric fields [27, 36–42]. Of these, AC electric fields are of particular interest since they are a facile means to remotely power the active particles, while their effects can be tuned through the parameters of the AC signal. In turn, this results in intriguing electrokinetic behaviors including propulsion, rotation, and particleparticle interactions [29,33,43,44]. Distinct electrokinetic mechanisms, e.g., electrohydrodynamic (EHD) flow [45–47], self-electrophoresis through diode rectification [48,49], induced charge electrophoresis (ICEP) [50,51], and self-dielectrophoresis (sDEP) [52], can be modulated by altering the field strength, frequency, and bias. Further, electrical actuation resolves the issue of finite energy supply associated with fuels, such as the commonly used hydrogen peroxide [53,54], and the challenge to manage chemical fuels in a biological environment. Additionally, it has been shown that the same electric actuation can be used simultaneously to accomplish both propulsion of active particles and manipulation of cargo, proving the robustness and versatility of AC electric energy [43].

The objective of this review is to highlight the key ideas and the recent progress in the electrohydrodynamic behavior of electrically powered active particles that are engineered in their shape, size, and materials composition. The last few years have seen great progress in the design and fabrication of particles of complex shape and composition. In the following sections, we first discuss various electrical field mechanisms that sustain and control the active motion of engineered particles, followed by elaboration on the aspects of engineered design. We then

examine diverse examples of engineered asymmetric colloids, their trajectories, and dynamic assembly behavior. Finally, we present a brief outlook on the current limitations, various applications, and future scope in active electrohydrodynamic systems.

2. AC-electric field effects in particle systems

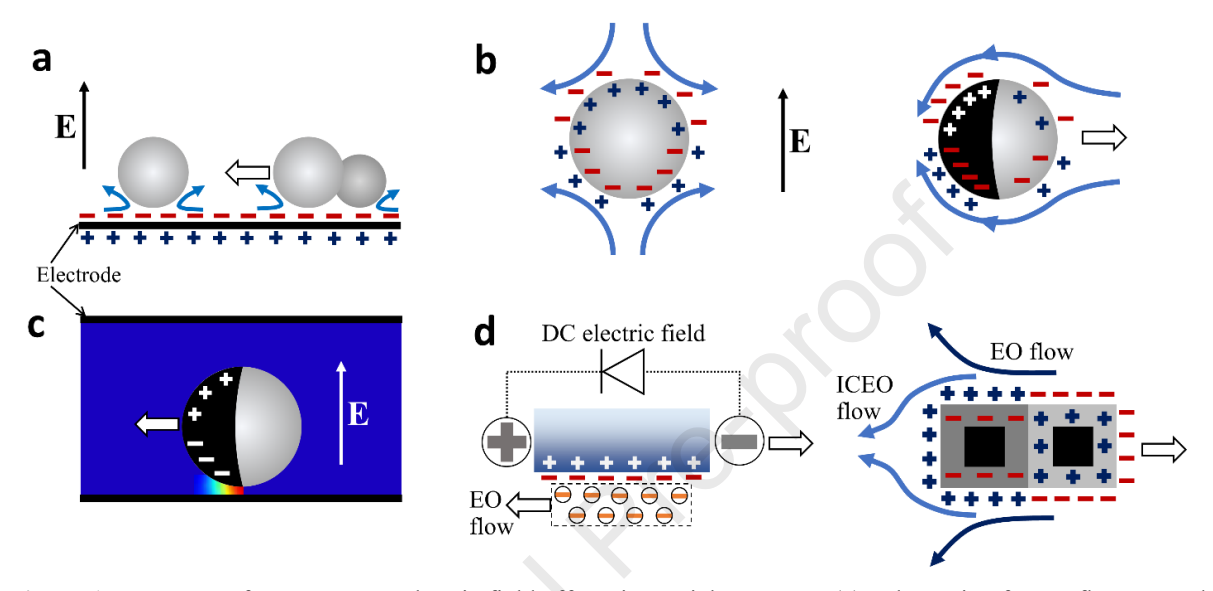


Figure 1. Summary of common AC-electric field effects in particle systems: (a) Schematic of EHD flow around a stationary spherical dielectric particle (left) and asymmetric dimer experiencing propulsion (right) in a vertical electric field. (b) Depiction of quadrupolar induced charge flow due to application of a steady state electric field that triggers the dipolar charges in the electrical double layer of the particle (left). A metallodielectric spherical particle with a hemispheric gold coating has asymmetric polarization (EDL around the gold is strongly polarized), resulting in induced charge electrophoretic motion (right). (c) As a result of dual symmetry breaking of a Janus sphere near a wall, a nonuniform field gradient interacts with the induced dipole in the metallic coating and generates a propulsion force with the metallic half forward, which occurs in the high frequency regime. d) A diode particle system and its equivalent electric circuit. Localized electroosmotic flow propels the particle due to the direct-current (DC) field rectified from an external AC electric field. ICEP and diode-based propulsion jointly propel the microparticle. ICEO flow and EO flow (due to diode generated DC field) are shown by arrows (right).

A particle subjected to an AC electric field can experience the effect of a few different electrohydrodynamic mechanisms based on the applied strength and frequency of the electric field (Figure 1). For a particle near the bottom electrode in a parallel-plate electrode configuration (Figure 1a), mobile charges are induced within the electrolyte interfacing the electrode, forming an induced electric double layer (EDL). The presence of the particle near the electrode disrupts the uniformity of the applied electric field and results in a tangential field component that acts on this induced EDL to generate EHD flow around the particles [47,55–59]. This flow causes either repulsion or aggregation of particles near the electrode surface and may also elevate the particles from the substrate [59,60]. The symmetric EHD flow around a symmetric particle (e.g., isotropic spherical particle) will not result in net particle motion. However, if the particles have asymmetry in the shape (e.g., two different sizes of lobes of a

colloidal dimer), an unbalanced flow surrounding the different lobes will generate a net motion (Figure 1a). EHD flow is generated at the lowest frequency regime in comparison to the ranges of frequencies for the other mechanisms. The characteristic frequency of the EHD is $f_{EHD} = D/(2\pi\lambda_o H)$, which corresponds to the charge relaxation time of the EDL induced at the electrolyte-electrode interface wherein λ_o is the Debye layer length, 2H the distance between electrodes and D the ionic diffusivity of the electrolyte (expressed here for the simplest case of a symmetric electrolyte, e.g. [47]). A maximum in the EHD effect is expected to occur around this frequency since for higher frequencies the induced EDL does not have time to be fully established, while for smaller frequencies the induced EDL screens the powered electrode and with it also the ability of the electric field to penetrate the microfluidic chamber [31,47]. The particle propulsion velocity is a function of the frequency as well as electric field strength ($U \propto E^2$). The speed and direction of motion can be altered by changing the geometry and anisotropy through variation of particle properties.

For a surface with fixed natural charges, the electric field that acts on the EDL results in tangential body force that generates linear electroosmotic (EO) flow [50,51,61]. In contrast, in a polarizable free solid particle, the non-uniform induced zeta potential leads to a non-linear electrokinetic phenomenon termed induced charge electroosmosis (ICEO), which acts on its own induced EDL. Particle velocity under this effect can again be scaled as $U \propto E^2$, although in some systems there is a tendency to transition towards linear behavior under high voltage fields [62]. The induced EDL is dipolar in nature and results in a quadrupolar flow (Figure 1b, left), which due to its symmetry does not lead to net motion of a freely suspended particle. However, introducing asymmetry in the system will distort the symmetrical quadrupolar ICEO flow and generate a net electrophoretic motion [2,63]. For spherically shaped particles, this is commonly realized by coating one of its halves with a metallic layer, thus forming a Janus particle. The more intense unbalanced ICEO flow on the metallic coated hemisphere results in net propulsion of the particle with its dielectric side forward (Figure 1b, right) in a direction that is perpendicular to the applied electric field [52]. The direction of motion is due to the orientation of the induced dipole along the metallodielectric interface (Figure 1b, right). The ICEO flow decays at frequencies beyond the charge relaxation time of the induced EDL, which is also known as the RC time for charging the double layer [51]. This flow can be expressed as f_{ICEO} = $D/(2\pi\lambda_0 a)$, where a is the characteristic particle's length scale. Beyond a certain frequency, the metallodielectric JP reverses direction with its metallic hemisphere forward. This effect, termed self-dielectrophoresis (sDEP), has been associated with a net electrostatic force that is generated in the high frequency regime where the induced EDLs on both the polarizable hemisphere of the JP as well as that on the powered electrode are partially screened (Figure 1c) [52]. Typical frequencies that were experimentally observed for a 5-10 µm metallo-dielectric JP within a low conductivity solution ($\sim 10^{-5}$ - 10^{-3} M KCl) are $f_{EHD} \sim 10$ -100Hz, $f_{ICEO} \sim 1$ -10kHz and reversal from ICEP to sDEP ~10-100kHz [31,52].

Yet another electrokinetic self-propelling mechanism stems from the internal asymmetry of the particle conductance. This can be achieved by using semiconductor diodes as particles in kind (Figure 1d, left). The diode particles rectify the applied external AC electric field by conducting in one direction only. The resulting DC electric field component between the electrodes of each diode drive electroosmotic ionic flow along the surface and lead to the particles' self-propulsion [48]. This mechanism can also be used to remotely power electrohydrodynamic diode pumps embedded in microfluidic devices [68].

3. Classes of particles that can exhibit AC-EHD

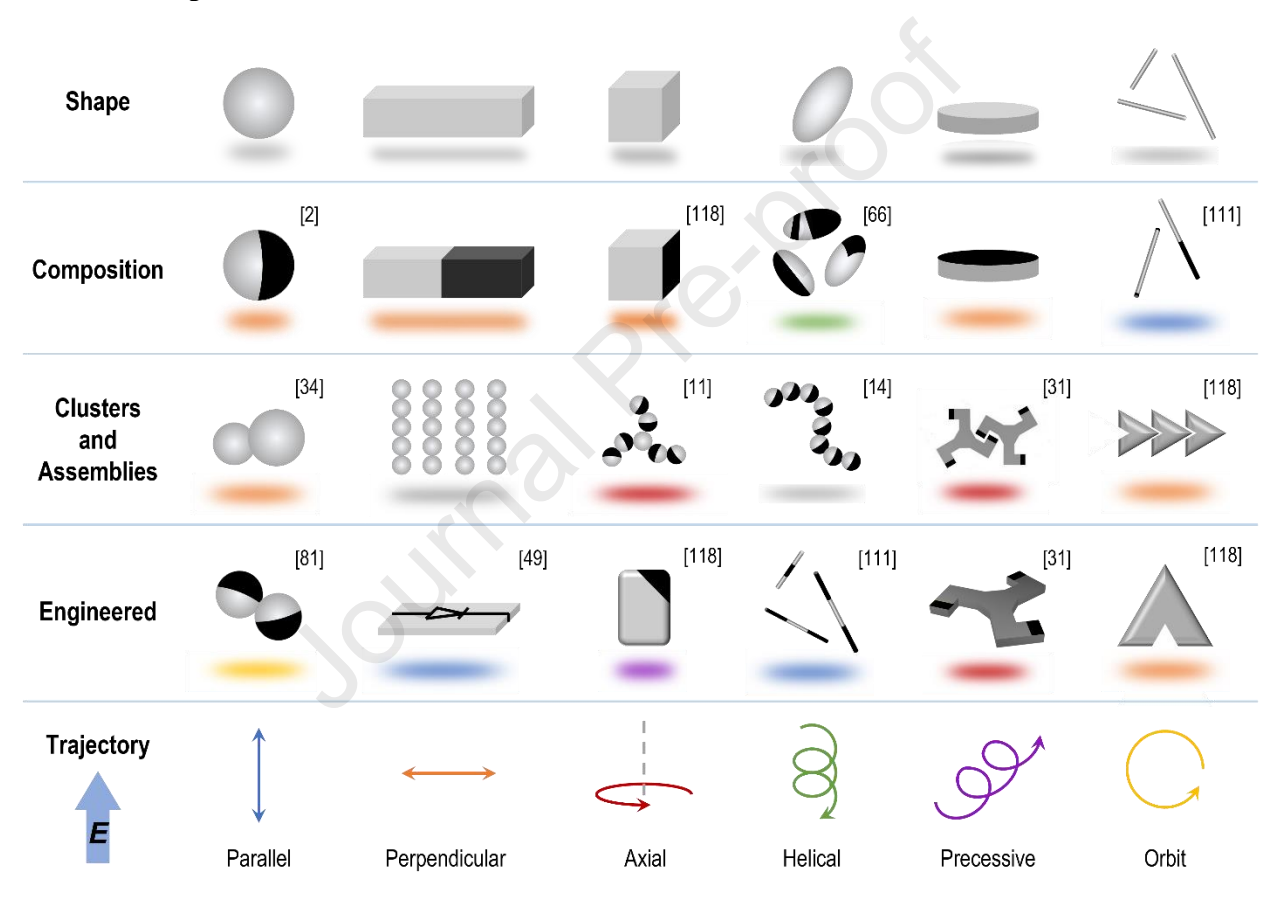


Figure 2. Tiered classification of particles that may exhibit AC-EHD motility. From top to bottom, particles can vary in shape, composition, number (via clusters and assemblies) and engineered design. These features, directing the EHD flows can produce a rich variety of trajectories. The color of the shadow under each unit corresponds to the color of its expected EHD-driven trajectory (bottom row). The trajectories row contains many of the most common examples but is not exhaustive.

Over the last several decades, we have seen the development of a rich variety of active particles that exhibit unique trajectories and behaviors as a result of AC-EHD effects. Due to the diverse particle features that contribute to these effects, it can be challenging to systematically analyze

the rich phenomena resulting from this. In this review, we present a system of classification for these particles in which complexity builds through the following tiers: shape, composition, number (via clusters and assemblies), and engineered design. A schematic of this classification with representative examples for each category is presented in Figure 2. This figure also presents the observed or expected types of corresponding trajectories. Some of these key particle classes will be reviewed in greater detail in later sections.

In understanding the effect of particle shape on AC field motility, one can consider the number of foci or vertices present as well as the distance and angle between these points, which effectively define the shape-based asymmetry of the particle. The localized AC-EHD effects at these points combine to induce various modes of particle motion. Particle anisotropy can also be varied through patches, coatings, and body composition, often resulting in a difference in polarizability between the regions. However, the trajectories evoked by simple shapes or coatings are often limited to linear-type motions. Incorporating asymmetry in both shape and composition can evolve trajectories into helical paths [20,66**]. Recent advances have made the transition from static field-driven assemblies to dynamic, multi-component active clusters, demonstrating behaviors such as rotation, flagellar motion, and linear trains [11,12,14,34]. These clusters and assemblies are generally comprised of individually active particles with attractive or interlocking interactions, leading to increasingly intricate EHD interactions within the larger group [28,31]. The modular nature of these clusters provides additional flexibility in design without the need for sophisticated fabrication techniques. However, such dynamic assemblies are still limited in complexity and shape. Thus, the final tier of our classification pertains to the engineered design and fabrication of more sophisticated AC-field propelled active particles.

The making of engineered active particles involves rational design of the structure along with moderate to high complexity in fabrication. For example, the fifth engineered particle in Figure 2 is a "supercolloidal spinner". This gear-like particle contains three arms, each with a metal patch near the tip, and was fabricated with lithographic techniques [31]. The spinner is designed with the intention of inducing EHD flow effects in multiple locations on the particle. The last row in Figure 2 presents the various trajectories one can expect to observe with AC field driven active particles, where the color of the shadows under each particle in the rows above matches the similarly colored trajectory. One additional degree of EHD-driven rotational motion can be observed by various types of Quincke rollers [69-73], but such DC-based systems fall outside the scope of this review on AC field-driven particles. All trajectories listed are derived from previously reported results, but one can imagine numerous other possible paths, such as undulatory waves, levitation, and flipping. We use this classification framework to review the parameters that affect AC EHD motion in the next section.

4. Motility of particles with engineered shape

4.1. Simple asymmetric particles

The simplest type of asymmetric particle is the Janus sphere, in which the two constituent hemispheres vary in composition [1]. Janus spheres have been designed to respond to a variety of stimuli, which may be magnetic, electric, light, acoustic, and chemical [1,67,74–80]. For the scope of this review, we discuss only those responsive to AC electric fields. Fabrication of electrically-responsive Janus spheres usually involves assembling a monolayer of dielectric (e.g., polystyrene (PS), silica) microbeads onto a substrate and then depositing on top of it a 20-30 nm layer of metal (e.g., Au, Pt, TiO₂, Cr, Fe₃O₄). The second step can be completed by a number of fabrication methods, including thermal evaporation, electron beam evaporation, glancing angle deposition (GLAD) and even microfluidic emulsification [2,20,81,82]. The mechanism of propulsion, at low to moderate (relative to the RC time) frequencies, originates from the imbalance in electroosmotic slip between the two differently polarizable hemispheres of the particle, as originally reported for Au-PS Janus spheres [2] (Figure 3a). Particle motion is in a direction perpendicular to the electric field lines and shows frequency-dependent direction switching. Due to their simple physical nature but complex behavior, Janus spheres have been the subject of many investigations of active particle propulsion and steering [5,9,51,81].

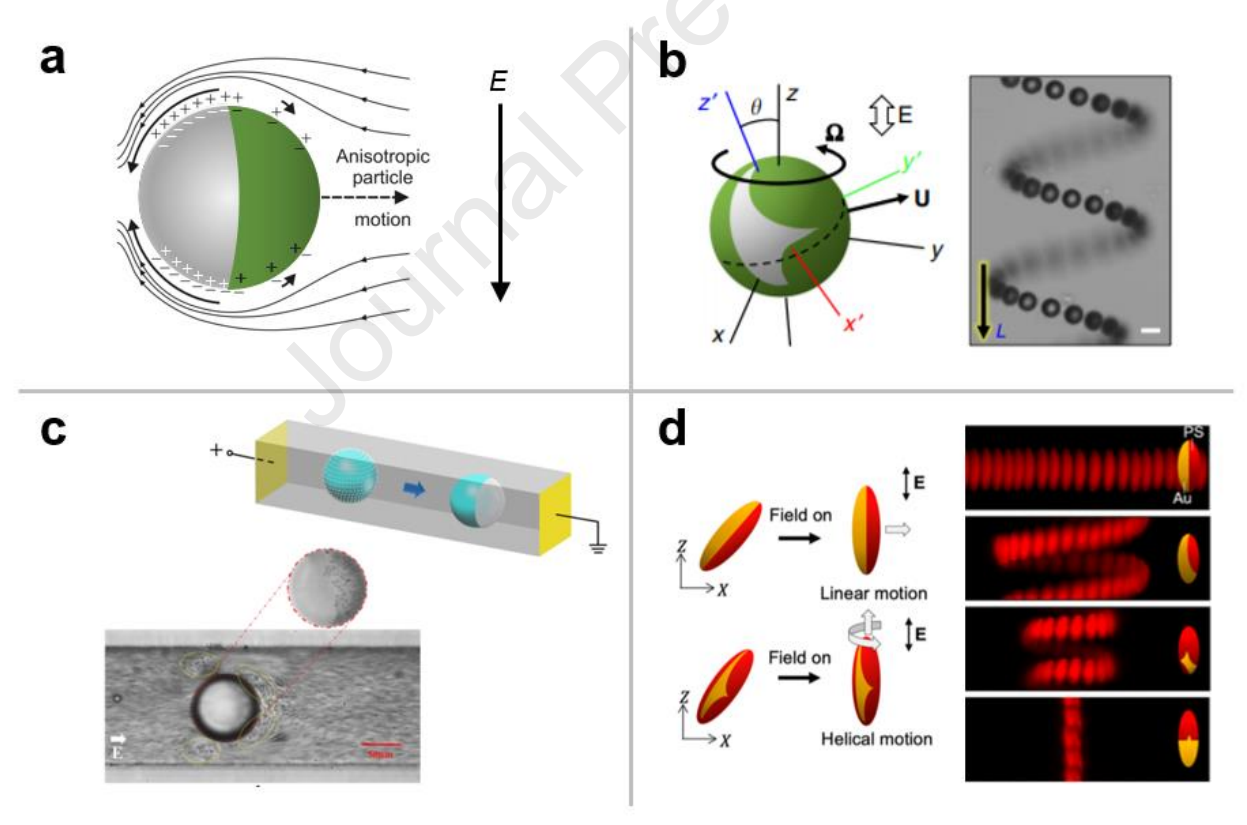


Figure 3. Key examples of Janus and other simple asymmetric particles that exhibit AC-EHD motility. (a) Schematic of ICEO flow in (EDL) of an Au-PS Janus particle with differently polarizable hemispheres; reprinted with permission from [2]. Copyright 2008, American Physical Society, (b) Schematic depicting axes of motion of patchy Au-PS spherical particle and superimposed brightfield micrographs showing corresponding 3-D helical trajectories; reprinted with permission from [20]. Adapted under the terms of a Creative Commons CC-BY license, (c) Microscope image of Janus oil droplet with Al₂O₃ nanoparticle half-shell and schematic of microfluidic chamber

used for its fabrication; reprinted with permission from [82]. Permission conveyed through Copyright Clearance Center, Inc., and (d) Schematic of patchy Au-PS ellipsoidal particles alongside superimposed brightfield micrographs showing corresponding trajectories based on patchy configuration; reprinted with permission from [66**]. Copyright 2021 American Chemical Society.

As an evolution to more complex anisotropy, Lee et al. fabricated via GLAD patchy spherical particles that move in helical, three-dimensional trajectories under an AC field (Figure 3b) [20]. This is an example of how complex trajectories can be encoded on a simple particle by shaping the patch on its surface. The patch orientation and size guide the EHD flows around the particles, leading to non-cylindrical helices and other programmed trajectories. Li and Li reported the microfluidic fabrication and field-driven behavior of Janus droplets in which positively charged, mobile Al₂O₃ nanoparticles comprised the hemispheric coating (Figure 3c) [82,83]. Upon exposure to a DC electric field, the nanoparticles collected on one side of the oil surface, rendering the droplet "Janus". This AC field-driven droplet behavior is attributed to ICEP and electroosmotic flows, both of which can be modulated by the degree of surface coverage with nanoparticles. Such a system offers another degree of flexibility in active particle surface morphology and consequent motility.

Patchy microellipsoids have also received attention as simple AC field-driven asymmetric particles capable of motility on complex trajectories. Lee et al. recently developed PS ellipsoidal microparticles with Au patches formed through thermal evaporation. Due to the layering of particles during evaporation, the patch configurations range from simple lengthwise Janus to angled and fragmented, resulting in both translational and helical ICEP motion (Figure 3d) [66**]. The motion patterns were shown to depend strongly on the degree of patch asymmetry along longitudinal and transverse axes. Another interesting study presented recently describes the motion of polyhedral particles based on Metal-Organic Frameworks (MOFs, [69]). These examples show how a multitude of EHD motion patterns can result from relatively simple asymmetric particles.

4.2. Doublets and multi-particle dynamic assemblies

Non-spherical particles come with many forms of anisotropy, such as dimers with two lobes. Many studies have reported directed assembly of symmetric/asymmetric doublets [84–88]. Wang et al. reported metal—organic hybrid dimers with various geometric variations and interfacial anisotropy [89]. EHD and ICEO flows control the self-propulsion of this dimer, with direction determined by solution conductivity (Figure 4a). For relatively high conductivities (1×10⁻⁴ M KCl), ICEO dominates over EHD flow and linear motion was exhibited with polystyrene lobes facing forward (Figure 4a, left). However, at lower conductivities (e.g., deionized water), EHD overcomes the ICEO flow and consequently, the metallic lobe moved forward. For the case of a dimer with identical chemical composition and size, but differing zeta potential, the dimer was observed to move with the lobe of lower zeta potential facing forward.

Boymelgreen et al. described the orbital motion of metallodielectric JP doublets (Figure 4b, left) under a uniform AC electric field [81]. The orbital motion was shown to depend on the relative orientations of the metallodielectric interfaces of the constituent JPs that form the doublet. The experimental results were explained using a heuristic kinematic rigid body model. Wirth and Nuthalapati theoretically revealed the interactions between a doublet of asymmetric zeta potential and size [92]. The doublet was influenced by two forces: (a) a net vertical force, which depends on lobe size and asymmetry in zeta potential and (b) a net lateral force perpendicular to the electric field, which depends on lobe size asymmetry, difference in zeta potential, and inclination angle of the doublet. The lateral motion of the doublet resulting from the net force was also perpendicular to the electric field. Apart from these forces, a net torque generated rotation of the doublet. These dimers are only capable of propelling along a direction perpendicular to the applied electric field. An active system in which the direction of propulsion is restricted to a single axis is problematic in many applications, such as directed cargo delivery.

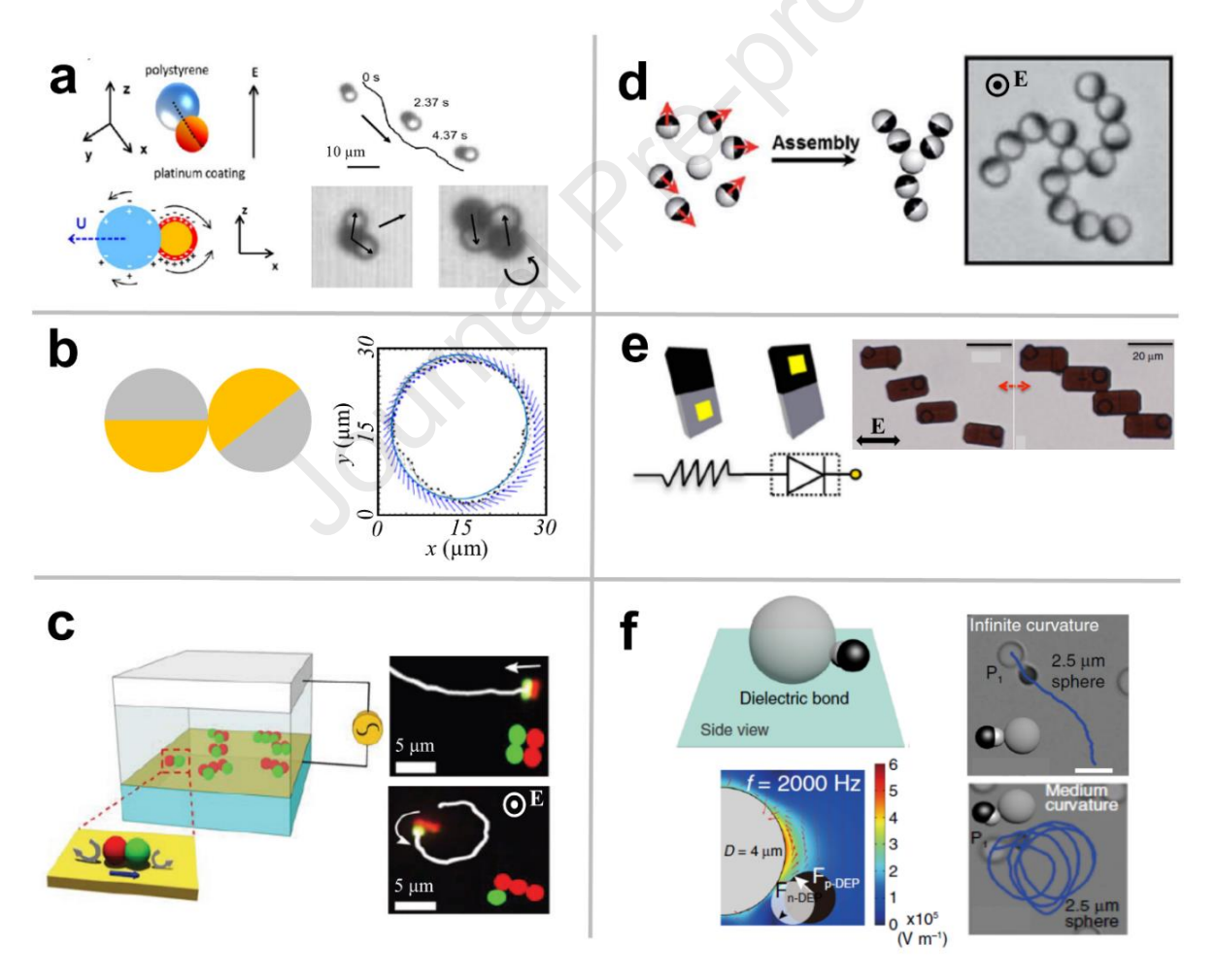


Figure 4. Examples of dynamic motion of colloidal dimers and assemblies under AC electric field actuation: (a) ICEO flow is generated due to difference in the polarizability of bare and platinum-coated polystyrene lobes. Dimer moves with bare polystyrene lobe forward. Dynamic motion of dimer clusters: Propulsion of two dimers with one common metallic lobe and rotation of head-to-tail dimer doublets (bottom right). Reprinted with permission

from [89]. Copyright 2014 American Chemical Society. (b) Schematic of a rigid body doublet. Results of kinematic model (solid blue lines) are compared to experimental data (dashed lines). Reprinted with permission from [81]. (c) Clusters fabricated by sCAPA. Inset depicts the configuration of colloidal molecules (CMs) with the direction of motion of surrounding fluid. Square-shaped cluster (top right) shows translation, while "L"-shaped cluster exhibits rotation (bottom right). Reprinted with permission from [90]. Permission conveyed through Copyright Clearance Center, Inc. Typical examples of multi-particle dynamic assemblies: (d) Schematic presentation of templated growth of chiral cluster. Chiral pinwheel undergoes clockwise motion. Reprinted with permission from [11]. Permission conveyed through Copyright Clearance Center, Inc. (e) Demonstration of PN-I type semiconductor particle and its equivalent electrical circuit diagram. Assembly (at 1 kHz, right) and disassembly (100 Hz, middle) of 4 PN-I microparticles using electrical signal; reprinted with permission from [65]. Adapted under the terms of a Creative Commons CC-BY license. (f) Formation of dielectric bond between central dielectric sphere and a patchy particle. Simulation shows that nDEP attraction leads to bonding between the sphere and the dielectric lobe and pDEP is responsible for metallic lobe bonding. Steering trajectories with infinite curvature (top right) and medium curvature (bottom right) of such colloidal molecules; reprinted with permission from [91*]. Adapted under the terms of a Creative Commons CC-BY license.

To address this concern, Zhu et al. investigated the motion of magnetic dimers synthesized under orthogonally applied AC electric and DC magnetic fields [93]. The magnetic field was used to orient the long axes of the dimers in the desired direction and concurrent application of an AC electric field was used to tune the speed. The combined actuation by magnetic and electric fields permits propulsion along a predefined complex trajectory with tunable speed. This strategy may allow future dynamic assembly of complex micromachines which exhibit controlled motion upon application of field gradients. Alapan et al. recently demonstrated the design and assembly of a modular micromachine frame with silica-gold Janus particle "actuators" [94**]. The non-uniform electric field gradients around the JPs generate ICEP and sDEP motions. By tuning the frequency of the field, these propulsion methods can interchange with each other, which can be used to design reconfigurable micromachines with a high degree of mobility. The described frame was applied to make a "microcar", in which different driving modes were made possible by altering the field parameters. This example suggests ways for modular design and multimodal control of future micromachines.

As mentioned earlier, multicomponent clusters show a high degree of broken symmetry which allows higher order tunability when compared with the propulsion and rotation of a single particle. Ni et al. fabricated clusters consisting of organic PS particles and inorganic TiO₂, SiO₂ particles using the sCAPA method [90]. These particle clusters showed complex translation, rotation, and circulation activated by asymmetric EHD flows (Figure 4c). The unbalanced EHD flows around a dumbbell-like colloidal molecule are shown in the inset of Figure 4c. Tuning the geometry and composition of the clusters enables pick-up and transport operations with a high degree of freedom and controllability.

Colloidal dimers can also form chiral clusters. Ma et al. reported how such chiral clusters can be formed by two/four in-plane dimers compacted closely with a central dimer on a conducting surface under an AC electric field [28]. Based on the theoretical analysis, induced dipolar interactions, which comprise (a) in-plane dipolar repulsive forces between the petals and (b) out-

of-plane attractive forces between the surrounding petals and central dimer, determined the cluster configuration. Asymmetric chiral clusters generated net EHD flow around the lobes, which induced rotational motion perpendicular to the applied electric field corresponding to their handedness. However, rotation was not found for achiral clusters because they generate a balanced EHD flow. Zhang and Granick presented a chiral, spiral shaped assembly of spherical Janus and homogeneous colloids under an AC electric field [11]. The electric field generates a dipole moment in the center of the uncoated silica particles and each hemisphere of the Janus particles. JPs exhibited head-to-tail attraction between the metallic and silica halves and hence, uncoated silica particles are attached to the metal hemispheres. Upon applying the electric field, spiral structures were formed with a bare silica particle as the core and three or four arms of JPs emanating from the core particle depending on its diameter (Figure 4d). The chiral structure generates self-sustaining rotation.

Recently, Ohiri et al. reported a novel set of motile semiconductor microparticles with varying shape, size, patterned coatings, and polarizability, made by microcircuit fabrication techniques [65*]. Figure 4e (left) depicts PN-I type semiconductor particles where electrical properties of the core silicon material were changed by diffusive patterning of a defined region. This process produces a p-n junction on a part of the particle. Under an AC electric field, a strong propulsive flow was generated toward the p-n junction and the metal contact due to combined effects of the rectifying junction and polarizable metal. The particle moved with the non-metal side facing forward. The metal patch generated anisotropic polarizations on the particle surface and the particle could also be propelled through strong ICEO flow, similar to metallodielectric JPs [2]. At relatively high frequencies, well-organized staggered chains were assembled due to dipolar polarization interactions between the particles (Figure 4e, right). The structure reversibly disassembles at lower frequencies (Figure 4e, middle).

Another notable example is the controlled dynamic interactions of patchy particles reported by Wang and coworkers [91*]. By manipulating composition, particle size, and shape, the authors coordinated and arranged the active particles into defined colloidal structures. Figure 4f shows a dielectrophoretic bond between a central dielectric sphere and a patchy particle. Positive DEP (pDEP) attraction is responsible for bonding the metallic lobe of the patchy particle, while negative DEP (nDEP) attraction favors the bonding between a dielectric sphere and dielectric lobe. When a metallodielectric patchy particle is bonded with the central dielectric sphere, the assembled doublet can swim and shows intriguing dynamics. For a bond angle of 90°, the patchy particle pushed the sphere and the assembly showed pure translational motion (Figure 4f, top right). However, when the bond angle was < 90°, the direction of motion of the patchy particle did not pass the mass center of the central particle, resulting in a steering motion of the assembly (Figure 4f, bottom right). The curvature of steering depends on bond angle, frequency of the AC signal, and shape of the patch.

4.3. Particle actuation and control with asymmetric and multiple fields

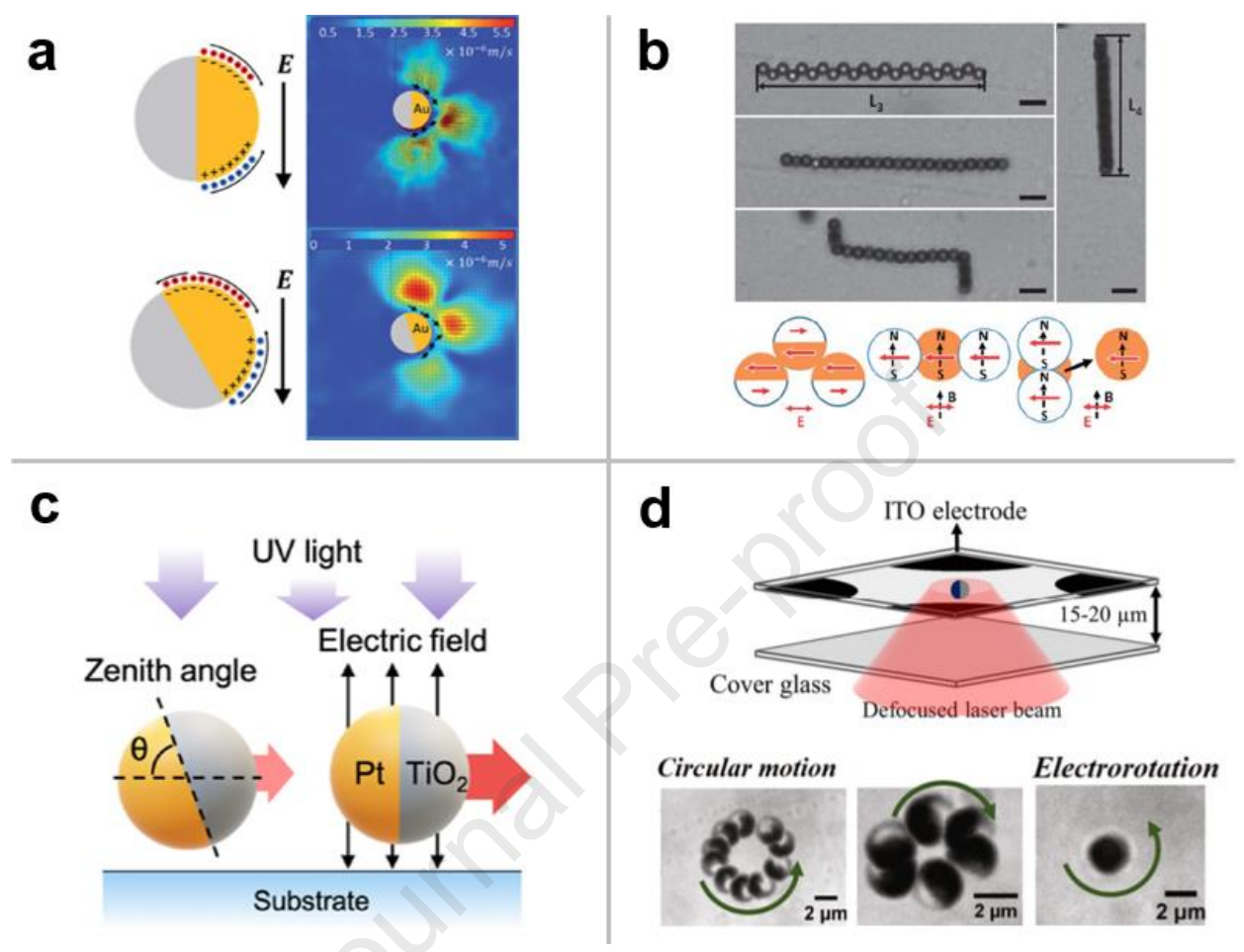


Figure 5. Recent examples of systems that can be controlled jointly by AC-EHD and other stimuli. (a) Coplanar multifield control of superparamagnetic Au-PS Janus particle and a visualization of the ICEP flow patterns as the orientation of the particle is adjusted via magnetic field; reprinted with permission from [15]. Permission conveyed through Copyright Clearance Center, Inc. (b) Chaining, bending, and reconfiguration of Fe₃O₄ Janus particles under combined AC electric and magnetic fields; reprinted with permission from [69]. Permission conveyed through Copyright Clearance Center, Inc. (c) Schematic of Pt-TiO₂ Janus particle exposed to AC field and UV light. Concurrent application of stimuli results in significant increase of speed; reprinted with permission from [97]. Copyright 2020 American Chemical Society. (d) Synergistic Janus particle rotation controlled by a defocused laser beam and rotating AC electric field. Below are brightfield microscopy images capturing the particle motion for combined fields below 2 kHz (left), 4-6 kHz (middle), and only rotating AC field (right); reprinted with permission from [98]. Adapted under the terms of a Creative Commons CC-BY license.

As the field of active particles shifts from fundamental exploration to application-based development, researchers are exploring the emergent field of multifunctional particles that are responsive to multiple field stimuli. Such particles can be subjected to two or more stimuli, either consecutively or simultaneously, to achieve outcomes that would not be realizable with a single field. These systems offer clear advantages over many current single-stimulus methods by increasing the particles' degrees of freedom and introducing new, nonlinear trajectories. To date,

there is a diverse array of multifunctional particles that respond to chemical, biological, magnetic, acoustic, and light-based stimuli [99–103,115]. In this section, we will highlight key examples of multi-field driven particle systems in which one component is AC field (Figure 5). In both cases below, the secondary field is compatible with the AC field in that it can be fixed precisely through variation of prescribed parameters (e.g., frequency, wavelength, intensity), resulting in reliable particle behavior with an extra degree of control over the competition between the two stimuli.

Combined application of magnetic and AC electric fields is a common strategy for field-directed assembly. Depending on the particle composition, induced magnetic dipoles can persist after the field is removed, whereas electric dipoles do not. Simultaneous magnetic and electric fields can also be employed to control single active particles. One key example is the coplanar multifield control of superparamagnetic Au-PS Janus particles in which the Au film thickness varies (Fig. 5a) [15]. It was found that 3 µm JPs with a thick, highly conductive and polarizable, Au shell (70 nm) demonstrated ICEP motion parallel to the electrodes, in contrast with previously reported thin-shell conditions. By introducing magnetic field manipulation of the particles' azimuthal orientation, Lin et al. were able to show the dependence of JP velocity with respect to the field on both coating thickness and dipole angle. Ruditskiy and coworkers reported results from Fe₃O₄-PS Janus particles under both parallel and perpendicular field geometry conditions (Fig. 5b) [69]. Such JPs were observed to form chains and contract in the first case, while instead the chains rotated and stacked into two-dimensional sheets under the second condition. Further, it has been shown that chain structure and dynamics is affected by the order in which the fields are applied.

Light is a simple and efficient stimulus that can be applied in a wide range of active systems. Micromotor activity resulting from optical stimulation can be predictably controlled due to the direct relationship to well-defined parameters, namely, wavelength and intensity. Entirely optically-driven active particles have been shown to exhibit a rich variety of behaviors, such as controlled flocking, scattering, and translational behavior [67,104,105]. Hybrid optical and electric active particles have great potential in multi-stimuli controlled systems. Recently, Xiao et al. reported findings of the nonlinear ICEP response of Pt-TiO₂ JPs when the particles were subjected simultaneously to an AC field (EHD) and UV light (photocatalysis of water) (Fig. 5c) [97]. It was observed that an individual particle's speed did not correspond to the sum of the speeds under single-stimulus conditions. This was attributed to the tilt rectification caused by the static AC field following the UV illumination. The combination of light and AC electric stimuli can not only affect particle velocity, but also trajectory. Chen and coworkers demonstrated a coupled multi-field effect in which circular motion of an Au-silica JP was modulated by concurrent application of a rotating AC electric field and a defocused laser beam [98]. Once subjected to a laser beam, these particles experience thermophoresis due to light absorption at the gold hemisphere. Combining this effect with a rotating AC electric field causes circular motion

of the particles, as opposed to simple electrorotation (Fig. 5d). Further, the rotation direction can be tuned by adjusting the frequency of the AC field signal. More recently, it was shown that navigation and steering of individual particles can be enhanced by including a focused laser beam to control orientation [106*]. Such synergistic effects are excellent examples of the complex outcomes possible in multi-stimulus active systems.

4.4. AC Propulsion of engineered particles

By engineering the shape of particles through microfabrications, researchers have achieved high degree of control over multiple motion mechanisms of active colloids. Shields et al. used photolithography and metal deposition techniques to fabricate complex patchy microspinners (Figure 6a) that exhibited tunable direction, speed, and switchable inversion in a uniform AC electric field [31]. The combination of discrete metallic patches on the body and complex shape of this patchy spinner made switchable use of four mechanisms, i.e., ICEO, sDEP, EHD, and reverse EHD, based on the ranges of frequency of the electric field. Through a series of scaling analyses, authors found that the frequency-controlled inversion in the rotation of nonpatchy microspinners was due to reversal in EHD flows. In addition, patchy microspinners changed the direction of rotation two more times at higher frequency owing to occurrence of ICEP flow and sDEP. Interaction between spinners could result in complicated locking (assembly) and unlocking (disassembly) behavior (Figure 6a, bottom right). Such locking and unlocking operations are useful in many systems, such as studying phase transitions [107,108].

Another way to fabricate complex active particles is the cluster-encapsulation-dewetting method. This method was developed by Wang and co-workers to fabricate patchy colloids of low-symmetry shapes [109*]. Particle geometry, size, and configurations of surface patches are key to underlying systems dynamics for controlled locomotion and assembly. Figure 6b (top row) shows a particle with two patches of different sizes located at the two ends of the particle [109*]. The ICEO flows generated from these patches act in opposition to each other. The stronger flow around the bigger patch pushes the particle forward. In such cases, the bigger patch generates the flow while the smaller patch acts as a brake. However, when patches are located asymmetrically, steering motion is generated due to semi-constructive ICEO flow of the two patches (Figure 6b, bottom row). In such a case, eccentricity is generated for an anisotropic particle and movement of the particle is due to the bigger patch; the smaller patch generates the torque required for steering. The trajectory and direction of steering depend on the location of the small patch.

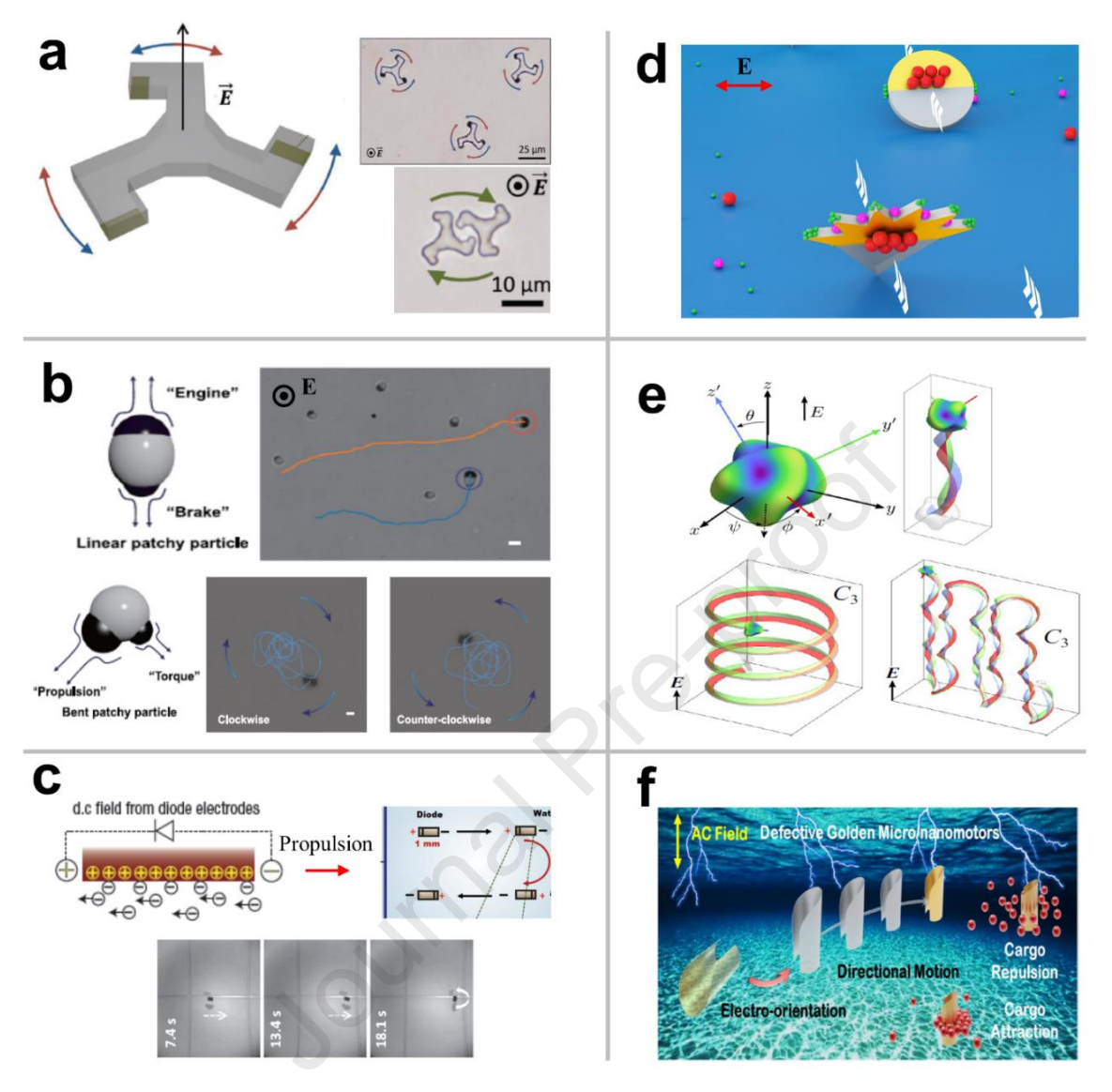


Figure 6. Representative examples of electrically powered engineered particles: (a) Schematic of supercolloidal spinner of polystyrene with gold coating at the distal ends of three arms. These spinners perform rotational motion under a vertical electric field. The particles exhibit locking at low electric field strength and unlocking (disassembly) at high electric field strength. Reprinted with permission from [31]. Permission conveyed through Copyright Clearance Center, Inc. (b) Linear translation of big-small two patch particle (top row) under an AC electric field. The big patch serves as an "engine" while small patch acts as a "brake". Steering of big-small two-patch particle (bottom row); reprinted with permission from [109*]. Copyright 2019 American Chemical Society. (c) Illustration of diode propulsion on water through electroosmosis generated due to DC voltage resulting from the rectification of applied AC field. Depiction of the process of diode steering (top right) and time sequences of diode propulsion and steering; reprinted with permission from [49]. Permission conveyed through Copyright Clearance Center, Inc. (d) Illustration of spike and disk-shaped engineered particle with cargo transport through pDEP and nDEP mechanisms. External AC electric field generates strong ICEO flow around the gold coating for overall propulsion and nonuniform field gradients at sharp corners generate DEP forces for cargo loading; reprinted with permission from [33]. Permission conveyed through Copyright Clearance Center, Inc. (e) A complex shape polarizable particle whose trajectory can be defined through alteration of its shape and symmetry. Helical trajectory of the complex particle (bottom left) and translation in a different direction of a wobbling cruiser (bottom right); reprinted with permission from [32]. (f) Time sequences of the propulsion of a "defective" golden micromotor. It shows electro-

orientation, directional motion, and cargo attraction/repulsion behavior; reprinted with permission from [110]. Permission conveyed through Copyright Clearance Center, Inc.

Semiconductor diodes also show self-propulsion by asymmetry of internal electrical conduction as already discussed previously. When an AC electric field is applied on the electrodes of millimeter-sized diodes, electro-osmotic flow is generated locally along the diode due to the rectification of the applied AC field [48]. The system was miniaturized by Calvo-Marzal and coworkers who used template electropolymerization and electrodeposition techniques to fabricate (PPy-Cd) nanowire diodes [111]. These authors showed the controllable propulsion of CdSe-Au-CdSe and PPy-Cd nanowire diodes driven by a uniform AC electric field. In using another set of effects in similar devices, Sharma and Velev reported how self-propelling microdiodes can be remotely controlled for on-demand steering (Figure 6c) [49]. The individual propulsion path of these electroosmotically driven diodes has been programmed electronically by modifying the applied AC signal. The steering was accomplished by incorporating a DC offset as a wave asymmetry into the AC signal, which generated electrostatic torque between the distribution of ionic charges and asymmetrically polarized diodes. The non-evenly distributed charges along the microdiode surface build up because of the capacitance of the double ionic layer. The authors present an equivalent circuit model and analyze the mechanism of the turning of a diode shown in Figure 6c. The use of a field-encoded DC offset as means of remote diode steering was analyzed and shown to work in a highly controllable and programmable manner [49].

The careful consideration of shape in designing engineered particles can significantly improve particle functionality and robustness. For example, in order to increase the number of cargo loading locations, Kunti et al. designed disk and spike-shaped engineered particles fabricated by a standard lithography process (Figure 6d) and actuated them using in-plane AC electric fields over an insulting substrate [33]. The spike-shaped active particles exhibited an enhanced cargo loading capability relative to the disk-shaped engineered Janus particles. In addition, the authors observed that varying the AC signal frequency and amplitude caused the particles to move tilt angle, reverse direction, and even flip. The tilt angle and flipping events are controlled mainly by ICEP and Maxwell stress tensor (MST) torques, where ICEP torque dominates in the lower frequency range and MST torque plays a major role at higher frequencies. The same group focused on modified metallodielectric pollen to enhance cargo loading capacity with different sizes of cargo [112]. Sharp corners of the pollen spikes generate sharp local gradients in the electric field and create multiple dielectrophoretic traps for cargo loading.

In a systematic study, Brooks et al. examined theoretically and numerically ICEP phenomena of particles with different symmetries (Figure 6e, top) and reported how particle shape can be used to program their numerous complex dynamic behaviors [32]. 3D analysis has been performed to identify translational and rotational trajectories allowed by symmetry. For each particular shape of a polarizable particle, the authors matched the specific dynamics using the numerical technique of boundary integral formulation containing hydrodynamic and electrostatic problems.

Apart from circular, translation, and rotational motion, analysis presented helical motion, oscillatory trajectories, and complex periodic orbits of the particles with specific corresponding shapes. The authors have shown how the particle trajectories can be modified through changes in their shape and asymmetry. Figure 6e (bottom images) shows two different trajectories: helical and zig-zag paths for a complex particle [32]. A helical trajectory was also seen for metallic and non-metallic microhelices in silicon oil media using a DC field [113]. This micromotor showed a cork-screw-type periodic rotation, the direction of which depends on its chirality (handedness).

Zhuang et al. investigated the dynamics of topologically defective asymmetric particles (Figure 6f) consisting of only one material (e.g., gold) [110]. Glancing angle deposition and membrane electrodeposition methods were used to fabricate active particles that circumvent the material constraints for the particle and substrate. Once the electric field is applied, this particle changes its orientation from horizontal to vertical and performs autonomous motion. Interaction between the electric field and the induced dipole on the thin coating (~50 nm) of the "defective" particle generate torque to align it along the field direction (vertical). The EDL around the particle is asymmetric because of its shape, resulting in a stronger EHD flow generated at the defect-free side as compared to the defective side in the ICEO regime. Such asymmetric particles can attract or repel various cargoes in a tunable way via altering signal frequencies.

5. Challenges and prospects

The fascinating dynamics of electrokinetically propelled engineered active particles is a topic of rapidly growing research interest. The recent progress in this area has been made possible by numerous strides in the advanced fabrication of engineered shaped particles [86,93]. Different methods, such as photolithography and physical metal deposition [31], sCAPA [90], clusterencapsulation-dewetting [109*], and dispersion polymerization [114] have been used to fabricate complex engineered particles, metallodielectric patchy particles, and colloidal molecules. Nevertheless, the reported fabrication strategies still face several challenges. It is difficult to find a sophisticated technique that enables large-scale, inexpensive production of precisely designed engineered particles. While recent years have seen large progress in the making of complex types of particles, the fundamental research in new propulsion mechanisms, such as the one induced by electric fields that are non-uniform either in space or in time, effect of asymmetric electrolytes [116], effect of multi-field actuation (e.g., thermophoresis [117] and electrokinetics [98]) still poses a number of interesting theoretical and computational challenges. In addition, the formulation of new techniques for directional navigation and steering remains an important challenge in the development of more complex active particle systems. There is a need to introduce steering approaches beyond the commonly used external magnetic fields that necessitate magnetic active particles. One nascent approach discussed here is to use the electrical signal itself as a means of providing encoded directional control [49,65*,118]. Another approach that is gaining popularity is using light illumination as means of steering of non-magnetic selfpropelling engineered particles by either introducing a photocatalytic effect [97,119] or a change in the electrical conductivity of a photo-responsive coated layer [120].

It is evident that complex active particles with pre-designed shape and composition-encoded functions can be driven by fundamental electrohydrodynamic effects, enabling to control their individual and collective behavior as well as interactions with each other in fluid medium. The academic interest in the electrically powered particle types discussed in this review has yet to result in investigations leading to the practical applications for these new classes of active systems. The complex dynamics and collective behavior of the engineered particles similar to the ones discussed here, integrated with different frequency-tunable electrokinetic mechanisms, open up new avenues in the field of active colloids. Particles with engineered propulsion and other functions can find applications in areas such as dynamic sensing, environmental remediation, detection and removal of cancer cells, in-vivo cargo delivery, insulin release, rapid cell apoptosis, oral vaccination, removal of pathogenic bacteria and toxins, and intracellular RNA delivery. The levels of complexity of such engineered structures are likely to keep increasing, while their design and implementation will be guided by the understanding of the numerous fundamental EHD effects reviewed here.

Declaration of competing interest

The authors declare that they have no known competing financial interests or personal relationships that could influence the work reported in this paper.

Acknowledgements

The authors gratefully acknowledge the financial support from BSF under grant 2018168, NSF under grant CBET 2133983, and partially NSF grant CBET 1935248.

References

Papers of particular interest, published within the period of review, have been highlighted as:

- * of special interest
- ** of outstanding interest
- [1] Walther A, Muller AHE. Janus particles: synthesis, self-assembly, physical properties, and applications. Chem Rev 2013;113:5194–261.
- [2] Gangwal S, Cayre OJ, Bazant MZ, Velev OD. Induced-charge electrophoresis of metallodielectric particles. Phys Rev Lett 2008;100:58302.
- [3] Boymelgreen AM, Miloh T. A theoretical study of induced-charge dipolophoresis of ideally polarizable asymmetrically slipping Janus particles. Phys Fluids 2011;23:72007.
- [4] Mano T, Delfau J-B, Iwasawa J, Sano M. Optimal run-and-tumble--based transportation of a Janus particle with active steering. Proc Natl Acad Sci 2017;114:E2580--E2589.
- [5] Zhang L, Xiao Z, Chen X, Chen J, Wang W. Confined 1D propulsion of metallodielectric Janus micromotors on microelectrodes under alternating current electric fields. ACS Nano 2019;13:8842–53.
- [6] Huo X, Wu Y, Boymelgreen A, Yossifon G. Analysis of Cargo Loading Modes and Capacity of

- an Electrically-Powered Active Carrier. Langmuir 2019.
- [7] Park S, Yossifon G. Micromotor-Based Biosensing Using Directed Transport of Functionalized Beads. ACS Sensors 2020;5:936–42.
- [8] Wu Y, Fu A, Yossifon G. Active particles as mobile microelectrodes for selective bacteria electroporation and transport. Sci Adv 2020;6:eaay4412.
- [9] Boymelgreen A, Yossifon G. Observing electrokinetic Janus particle--channel wall interaction using microparticle image velocimetry. Langmuir 2015;31:8243–50.
- [10] Nishiguchi D, Sano M. Mesoscopic turbulence and local order in Janus particles self-propelling under an ac electric field. Phys Rev E 2015;92:52309.
- [11] Zhang J, Granick S. Natural selection in the colloid world: active chiral spirals. Faraday Discuss 2016;191:35–46.
- [12] Zhang J, Yan J, Granick S. Directed self-assembly pathways of active colloidal clusters. Angew Chemie 2016;128:5252–5.
- [13] Yan J, Han M, Zhang J, Xu C, Luijten E, Granick S. Reconfiguring active particles by electrostatic imbalance. Nat Mater 2016;15:1095–9.
- [14] Nishiguchi D, Iwasawa J, Jiang H-R, Sano M. Flagellar dynamics of chains of active Janus particles fueled by an AC electric field. New J Phys 2018;20:15002.
- [15] Lin C-H, Chen Y-L, Jiang H-R. Orientation-dependent induced-charge electrophoresis of magnetic metal-coated Janus particles with different coating thicknesses. RSC Adv 2017;7:46118–23
- [16] Demirörs AF, Eichenseher F, Loessner MJ, Studart AR. Colloidal shuttles for programmable cargo transport. Nat Commun 2017;8:1–7.
- [17] Loget G, Kuhn A. Bulk synthesis of Janus objects and asymmetric patchy particles. J Mater Chem 2012;22:15457–74.
- [18] Rodríguez-Fernández D, Liz-Marzán LM. Metallic Janus and patchy particles. Part Part Syst Charact 2013;30:46–60.
- [19] Kretzschmar I, Song JHK. Surface-anisotropic spherical colloids in geometric and field confinement. Curr Opin Colloid Interface Sci 2011;16:84–95.
- [20] Lee JG, Brooks AM, Shelton WA, Bishop KJM, Bharti B. Directed propulsion of spherical particles along three dimensional helical trajectories. Nat Commun 2019;10:1–8.
- [21]* Li W, Palis H, Merindol R, Majimel J, Ravaine S, Duguet E. Colloidal molecules and patchy particles: Complementary concepts, synthesis and self-assembly. Chem Soc Rev 2020;49:1955–76.
 - Thorough review of fabrication techniques and areas of application of both organic and inorganic colloidal building blocks.
- [22] Bianchi E, Capone B, Coluzza I, Rovigatti L, van Oostrum PDJ. Limiting the valence: advancements and new perspectives on patchy colloids, soft functionalized nanoparticles and biomolecules. Phys Chem Chem Phys 2017;19:19847–68.
- [23] Ravaine S, Duguet E. Synthesis and assembly of patchy particles: Recent progress and future prospects. Curr Opin Colloid Interface Sci 2017;30:45–53.
- [24] Rozynek Z, Józefczak A. Patchy colloidosomes--an emerging class of structures. Eur Phys J Spec Top 2016;225:741–56.
- [25] Solomon MJ. Directions for targeted self-assembly of anisotropic colloids from statistical thermodynamics. Curr Opin Colloid Interface Sci 2011;16:158–67.
- [26] Zhang J, Luijten E, Grzybowski BA, Granick S. Active colloids with collective mobility status and research opportunities. Chem Soc Rev 2017;46:5551–69.
- [27] Orozco J, Cheng G, Wang J, Vilela D, Sattayasamitsathit S, Vazquez-Duhalt R, et al. Micromotor-Based High-Yielding Fast Oxidative Detoxification of Chemical Threats. Angew Chemie Int Ed 2013;52:13276–9.
- [28] Ma F, Wang S, Wu DT, Wu N. Electric-field--induced assembly and propulsion of chiral colloidal

- clusters. Proc Natl Acad Sci 2015;112:6307-12.
- [29] Kümmel F, Ten Hagen B, Wittkowski R, Buttinoni I, Eichhorn R, Volpe G, et al. Circular motion of asymmetric self-propelling particles. Phys Rev Lett 2013;110:198302.
- [30] Brooks AM, Tasinkevych M, Sabrina S, Velegol D, Sen A, Bishop KJM. Shape-directed rotation of homogeneous micromotors via catalytic self-electrophoresis. Nat Commun 2019;10:1–9.
- [31] Shields IV CW, Han K, Ma F, Miloh T, Yossifon G, Velev OD. Supercolloidal spinners: Complex active particles for electrically powered and switchable rotation. Adv Funct Mater 2018;28:1803465.
- [32] Brooks AM, Sabrina S, Bishop KJM. Shape-directed dynamics of active colloids powered by induced-charge electrophoresis. Proc Natl Acad Sci 2018;115:E1090--E1099.
- [33]** Kunti G, Wu Y, Yossifon G. Rational Design of Self- Propelling Particles for Unified Cargo Loading and Transportation. Small 2021:2007819.

 Experimentally observed engineered particles exhibiting a tilt angle, flipping and cargo loading under an in-plane electric field
- [34] Ma F, Yang X, Zhao H, Wu N. Inducing propulsion of colloidal dimers by breaking the symmetry in electrohydrodynamic flow. Phys Rev Lett 2015;115:208302.
- [35] Abbott NL, Velev OD. Active particles propelled into researchers' focus. Curr. Opinion Colloid Interface Sci 2016;21:1-3.
- [36] Guix M, Mayorga-Martinez CC, Merkoçi A. Nano/micromotors in (bio) chemical science applications. Chem Rev 2014;114:6285–322.
- [37]* Liljeström V, Chen C, Dommersnes P, Fossum JO, Gröschel AH. Active structuring of colloids through field-driven self-assembly. Curr Opin Colloid Interface Sci 2019;40:25–41. Comprehensive review of active self-assembly that discusses both static and non-equilibrium states for electric, magnetic, and optical stimulation.
- [38] Wang H, Pumera M. Fabrication of micro/nanoscale motors. Chem Rev 2015;115:8704–35.
- [39]* Driscoll M, Delmotte B. Leveraging collective effects in externally driven colloidal suspensions: Experiments and simulations. Curr Opin Colloid Interface Sci 2019;40:42–57. Extensive review of theoretical and experimental work in understanding the hydrodynamic mechanisms at play in magnetic, electric, and acoustically-driven colloidal systems.
- [40] Ebbens SJ, Howse JR. In pursuit of propulsion at the nanoscale. Soft Matter 2010;6:726–38.
- [41] Xu T, Gao W, Xu L-P, Zhang X, Wang S. Fuel-free synthetic micro-nanomachines. Adv Mater 2017;29:1603250.
- [42] Bouffier L, Ravaine V, Sojic N, Kuhn A. Electric fields for generating unconventional motion of small objects. Curr Opin Colloid Interface Sci 2016;21:57–64.
- [43] Boymelgreen AM, Balli T, Miloh T, Yossifon G. Active colloids as mobile microelectrodes for unified label-free selective cargo transport. Nat Commun 2018;9:1–8.
- [44] Velev OD, Bhatt KH. On-chip micromanipulation and assembly of colloidal particles by electric fields. Soft Matter 2006;2:738–50.
- [45] Trau M, Saville DA, Aksay IA. Field-induced layering of colloidal crystals. Science (80-) 1996;272:706–9.
- [46]** Yang X, Johnson S, Wu N. The Impact of Stern-Layer Conductivity on the Electrohydrodynamic Flow Around Colloidal Motors under an Alternating Current Electric Field. Adv Intell Syst 2019;1:1900096.
 Insightful study elucidating the fundamental mechanisms behind extensile and contractile EHD flows in systems of varying zeta potentials.
- [47] Ristenpart WD, Jiang P, Slowik MA, Punckt C, Saville DA, Aksay IA. Electrohydrodynamic flow and colloidal patterning near inhomogeneities on electrodes. Langmuir 2008;24:12172–80.

- [48] Chang ST, Paunov VN, Petsev DN, Velev OD. Remotely powered self-propelling particles and micropumps based on miniature diodes. Nat Mater 2007;6:235–40.
- [49] Sharma R, Velev OD. Remote Steering of Self-Propelling Microcircuits by Modulated Electric Field. Adv Funct Mater 2015;25:5512–9.
- [50] Squires TM, Bazant MZ. Induced-charge electro-osmosis. J Fluid Mech 2004;509:217–52.
- [51] Squires TM, Bazant MZ. Breaking symmetries in induced-charge electro-osmosis and electrophoresis. J Fluid Mech 2006;560:65–101.
- [52] Boymelgreen A, Yossifon G, Miloh T. Propulsion of active colloids by self-induced field gradients. Langmuir 2016;32:9540–7.
- [53] Wang W, Duan W, Ahmed S, Mallouk TE, Sen A. Small power: Autonomous nano- and micromotors propelled by self-generated gradients. Nano Today 2013;8:531–54.
- [54] Ebbens SJ. Active colloids: Progress and challenges towards realising autonomous applications. Curr Opin Colloid Interface Sci 2016;21:14–23.
- [55] Trau M, Saville DA, Aksay IA. Assembly of colloidal crystals at electrode interfaces. Langmuir 1997;13:6375–81.
- [56] Ristenpart WD, Aksay IA, Saville DA. Assembly of colloidal aggregates by electrohydrodynamic flow: Kinetic experiments and scaling analysis. Phys Rev E 2004;69:21405.
- [57] Ristenpart WD, Aksay IA, Saville DA. Electrohydrodynamic flow around a colloidal particle near an electrode with an oscillating potential. J Fluid Mech 2007;575:83–109.
- [58] Ristenpart WD, Aksay IA, Saville DA. Electrically driven flow near a colloidal particle close to an electrode with a faradaic current. Langmuir 2007;23:4071–80.
- [59] Fagan JA, Sides PJ, Prieve DC. Mechanism of rectified lateral motion of particles near electrodes in alternating electric fields below 1 kHz. Langmuir 2006;22:9846–52.
- [60] Woehl TJ, Chen BJ, Heatley KL, Talken NH, Bukosky SC, Dutcher CS, et al. Bifurcation in the Steady-State Height of Colloidal Particles near an Electrode in Oscillatory Electric Fields: Evidence for a Tertiary Potential Minimum. Phys Rev X 2015;5:11023.
- [61] Laser DJ, Myers AM, Yao S, Bell KF, Goodson KE, Santiago JG, et al. Silicon electroosmotic micropumps for integrated circuit thermal management. TRANSDUCERS'03. 12th Int. Conf. Solid-State Sensors, Actuators Microsystems. Dig. Tech. Pap. (Cat. No. 03TH8664), vol. 1, 2003, p. 151–4.
- [62] Shnitzer O, Yariv E, Strong-field electrophoresis. J Fluid Mech 2012;701:333-351.
- [63] Gangwal S, Cayre OJ, Velev OD. Dielectrophoretic assembly of metallodielectric Janus particles in AC electric fields. Langmuir 2008;24:13312–20.
- [64] Miloh T. Dipolophoresis of interacting conducting nano-particles of finite electric double layer thickness. Phys Fluids 2011;23:122002.
- [65]* Ohiri U, Shields CW, Han K, Tyler T, Velev OD, Jokerst N. Reconfigurable engineered motile semiconductor microparticles. Nat Commun 2018;9:1–9.
 Microfabrication of micron-scale semincoductor diodes with different metallo-dielectric configurations allows making of multiple classes of self-propelling microdevices with various motility and DEP aseembly modes.
- [66]** Lee JG, Al Harraq A, Bishop KJM, Bharti B. Fabrication and Electric Field-Driven Active Propulsion of Patchy Microellipsoids. J Phys Chem B 2021;125:4232–40. First report of active AC field-driven microellipsoids. This is also one of only two reports of 3D helical trajectories caused by simple patch geometry.
- [67] Dong R, Zhang Q, Gao W, Pei A, Ren B. Highly efficient light-driven TiO2--Au Janus micromotors. ACS Nano 2016;10:839–44.
- [68] Chang ST, Paunov VN, Petsev DN, Velev OD. Remotely powered self-propelling particles and micropumps based on miniature diodes. Nat Mater 2007; 235-40.
- [69] Wang Z, Xu W, Wang Z, Lyu D, Mu Y, Duan W, et al., Polyhedral Micromotors of Metal--Organic

- Frameworks: Symmetry Breaking and Propulsion. J Am Chem Soc 2021;143:19881–92.
- [70] Han E, Zhu L, Shaevitz J, Stone H, Low-Reynolds-number, biflagellated Quincke swimmers with multiple forms of motion. P Natl Acad Sci USA 2021; 2105.04096.
- [71] Pradillo GE, Karani H, Vlahovska PM, Quincke rotor dynamics in confinement: rolling and hovering. Soft Matter 2019;15:6564-6570.
- [72] Bricard A, Caussin JB, Desreumaux N, Dauchot O, Bartolo D, Emergence of macroscopic directed motion in populations of motile colloids. Nature 2013;503: 95–98.
- [73] Bricard A, Caussin JB, Das D, Savoie C, Vijayakumar C, Kyohei S, et al., Emergent vortices in populations of colloidal rollers. Nat Commun 2015;6:7470.
- [74] Ruditskiy A, Ren B, Kretzschmar I. Behaviour of iron oxide (Fe 3 O 4) Janus particles in overlapping external AC electric and static magnetic fields. Soft Matter 2013;9:9174–81.
- [75] Guix M, Meyer AK, Koch B, Schmidt OG. Carbonate-based Janus micromotors moving in ultralight acidic environment generated by HeLa cells in situ. Sci Rep 2016;6:1–7.
- [76] Gao W, Pei A, Dong R, Wang J. Catalytic iridium-based Janus micromotors powered by ultralow levels of chemical fuels. J Am Chem Soc 2014;136:2276–9.
- [77] Valdez-Garduño M, Leal-Estrada M, Oliveros-Mata ES, Sandoval-Bojorquez DI, Soto F, Wang J, et al. Density Asymmetry Driven Propulsion of Ultrasound-Powered Janus Micromotors. Adv Funct Mater 2020;30:2004043.
- [78] Zhang X, Fu Q, Duan H, Song J, Yang H. Janus Nanoparticles: From Fabrication to (Bio) Applications. ACS Nano 2021;15:6147–91.
- [79] Mou F, Chen C, Ma H, Yin Y, Wu Q, Guan J. Self-Propelled Micromotors Driven by the Magnesium--Water Reaction and Their Hemolytic Properties. Angew Chemie Int Ed 2013;52:7208–12.
- [80] Chen C, Mou F, Xu L, Wang S, Guan J, Feng Z, et al. Light-Steered Isotropic Semiconductor Micromotors. Adv Mater 2017;29:1603374.
- [81] Boymelgreen A, Yossifon G, Park S, Miloh T. Spinning Janus doublets driven in uniform ac electric fields. Phys Rev E 2014;89:11003.
- [82] Li M, Li D. Fabrication and electrokinetic motion of electrically anisotropic Janus droplets in microchannels. Electrophoresis 2017;38:287–95.
- [83] Li M, Li D. Janus droplets and droplets with multiple heterogeneous surface strips generated with nanoparticles under applied electric field. J Phys Chem C 2018;122:8461–72.
- [84] Ma F, Wang S, Smith L, Wu N. Two-dimensional assembly of symmetric colloidal dimers under electric fields. Adv Funct Mater 2012;22:4334–43.
- [85] Demirors AF, Johnson PM, van Kats CM, van Blaaderen A, Imhof A. Directed self-assembly of colloidal dumbbells with an electric field. Langmuir 2010;26:14466–71.
- [86] Panczyk MM, Park J-G, Wagner NJ, Furst EM. Two-dimensional directed assembly of dicolloids. Langmuir 2013;29:75–81.
- [87] Hosein ID, Lee SH, Liddell CM. Dimer-based three-dimensional photonic crystals. Adv Funct Mater 2010;20:3085–91.
- [88] Hernández-Navarro S, Ignes-Mullol J, Sagues F, Tierno P. Role of anisotropy in electrodynamically induced colloidal aggregates. Langmuir 2012;28:5981–6.
- [89] Wang S, Ma F, Zhao H, Wu N. Bulk Synthesis of Metal--Organic Hybrid Dimers and Their Propulsion under Electric Fields. ACS Appl Mater Interfaces 2014;6:4560–9.
- [90] Ni S, Marini E, Buttinoni I, Wolf H, Isa L. Rational design and fabrication of versatile active colloidal molecules. ArXiv Prepr ArXiv170108061 2017.
- [91]* Wang Z, Wang Z, Li J, Tian C, Wang Y. Active colloidal molecules assembled via selective and directional bonds. Nat Commun 2020;11:1–12.

 Fundamental investigation into the representation of active particles as molecules with emphasis on the flexibility of this modular scheme. Various configurations of active molecules can yield diverse navigation and steering outcomes.

- [92] Wirth CL, Nuthalapati SH. Response of a doublet to a nearby dc electrode of uniform potential. Phys Rev E 2016;94:42614.
- [93] Zhu X, Gao Y, Mhana R, Yang T, Hanson BL, Yang X, et al. Synthesis and Propulsion of Magnetic Dimers under Orthogonally Applied Electric and Magnetic Fields. Langmuir 2021.
- [94]** Alapan Y, Yigit B, Beker O, Demirörs AF, Sitti M. Shape-encoded dynamic assembly of mobile micromachines. Nat Mater 2019;18:1244–51.
 First report of reconfigurable, self-assembled AC field-driven modular micromachine. Establishes the foundation for possible development of microrobots in the future.
- [95] Yang X, Wu N. Change the collective behaviors of colloidal motors by tuning electrohydrodynamic flow at the subparticle level. Langmuir 2018;34:952–60.
- [96] Ohiri U, Han K, Shields IV CW, Velev OD, Jokerst NM. Propulsion and assembly of remotely powered p-type silicon microparticles. APL Mater 2018;6:121102.
- [97] Xiao Z, Duan S, Xu P, Cui J, Zhang H, Wang W. Synergistic Speed Enhancement of an Electric-Photochemical Hybrid Micromotor by Tilt Rectification. ACS Nano 2020;14:8658–67.
- [98] Chen Y, Yang C, Jiang H. Electrically enhanced self-thermophoresis of laser-heated Janus particles under a rotating electric field. Sci Rep 2018;8:5945.
- [99] Kirillova A, Marschelke C, Synytska A. Hybrid Janus particles: challenges and opportunities for the design of active functional interfaces and surfaces. ACS Appl Mater Interfaces 2019;11:9643–71
- [100] Gao W, Feng X, Pei A, Gu Y, Li J, Wang J. Seawater-driven magnesium based Janus micromotors for environmental remediation. Nanoscale 2013;5:4696–700.
- [101] Komazaki Y, Hirama H, Torii T. Electrically and magnetically dual-driven Janus particles for handwriting-enabled electronic paper. J Appl Phys 2015;117:154506.
- [102] Ren L, Zhou D, Mao Z, Xu P, Huang TJ, Mallouk TE. Rheotaxis of bimetallic micromotors driven by chemical--acoustic hybrid power. ACS Nano 2017;11:10591–8.
- [103] Celik Cogal G, Das PK, Li S, Uygun Oksuz A, Bhethanabotla VR. Unraveling the Autonomous Motion of Polymer-Based Catalytic Micromotors Under Chemical- Acoustic Hybrid Power. Adv NanoBiomed Res 2021;1:2000009.
- [104] Choudhury U, Singh DP, Qiu T, Fischer P. Chemical nanomotors at the gram scale form a dense active optorheological medium. Adv Mater 2019;31:1807382.
- [105] Mou F, Zhang J, Wu Z, Du S, Zhang Z, Xu L, et al. Phototactic flocking of photochemical micromotors. Iscience 2019;19:415–24.
- [106]* Peng X, Chen Z, Kollipara PS, Liu Y, Fang J, Lin L, et al. Opto-thermoelectric microswimmers. Light Sci Appl 2020;9:141.

 Extension of new fundamental knowledge regarding the role of thermophoresis in creating electric field gradients and use of focused and defocused laser beams to induce multiple modes of motion.
- [107] Nguyen NHP, Klotsa D, Engel M, Glotzer SC. Emergent collective phenomena in a mixture of hard shapes through active rotation. Phys Rev Lett 2014;112:75701.
- [108] Spellings M, Engel M, Klotsa D, Sabrina S, Drews AM, Nguyen NHP, et al. Shape control and compartmentalization in active colloidal cells. Proc Natl Acad Sci 2015;112:E4642--E4650.
- [109]* Wang Z, Wang Z, Li J, Cheung STH, Tian C, Kim S-H, et al. Active patchy colloids with shape-tunable dynamics. J Am Chem Soc 2019;141:14853–63.
 Significant contribution to the navigation and steering of active particles. Authors present a simple and elegant solution to a major challenge in the field.
- [110] Zhuang R, Zhou D, Chang X, Mo Y, Zhang G, Li L. Alternating Current Electric Field Driven Topologically Defective Micro/nanomotors. Appl Mater Today 2022;26:101314
- [111] Calvo-Marzal P, Sattayasamitsathit S, Balasubramanian S, Windmiller JR, Dao C, Wang J.

- Propulsion of nanowire diodes. Chem Commun 2010;46:1623-4.
- [112] Park S, Finkelman L, Yossifon G. Enhanced cargo loading of electrically powered metallodielectric pollen bearing multiple dielectrophoretic traps. J Colloid Interface Sci 2021;588:611–8.
- [113] Yamamoto D, Kosugi K, Hiramatsu K, Zhang W, Shioi A, Kamata K, et al. Helical micromotor operating under stationary DC electrostatic field. J Chem Phys 2019;150:14901.
- [114] Zhu B, Fei C, Wang C, Zhu Y, Yang X, Zheng H, et al. Self-focused AlScN film ultrasound transducer for individual cell manipulation. ACS Sensors 2017;2:172–7.
- [115] Zhang S, Shakiba N, Chen Y, Zhang Y, Tian P, Singh J, et al. Patterned optoelectronic tweezers: A new scheme for selecting, moving, and storing dielectric particles and cells. Small 2018;14:1803342.
- [116] Miloh T, Nagler J. Electrorotation of leaky-dielectric and conducting microspheres in asymmetric electrolytes and angular velocity reversal. Electrophoresis 2020;41:1296-1307.
- [117] Miloh T, Nagler J. Light-induced self-thermophoresis of Janus spheroidal nanoparticles. Electrophoresis 2018;39: 2417-2424.
- [118] Han K, Shields IV CW, Velev OD. Engineering of self- propelling microbots and microdevices powered by magnetic and electric fields. Adv Funct Mater 2018;1705953:1-14.
- [119] Chen X, Zhou C, Peng Y, Wang Q, Wang W. Temporal light modulation of photochemically active, oscillating micromotors: dark pulses, mode switching, and controlled clustering. ACS Appl Mater Interf, 2020;12:11843-51.
- [120] Soma R, Nakayama B, Kuwahara M, Yamamoto E, Saiki T. Phase-change Janus particles with switchable dual properties. Appl Phys Lett 2020;117:221601.

Journal Pre-proof

Declaration of interests

☑The authors declare that they have no known competing financial interests or personal relationship
that could have appeared to influence the work reported in this paper.

☐The authors declare the following financial interests/personal relationships which may be considered as potential competing interests: